[CANCER RESEARCH 63, 5401–5407, September 1, 2003]

TR3/Nur77 in Colon Cancer Cell Apoptosis[1]

Andrew J. Wilson,[2] Diego Arango, John M. Mariadason, Barbara G. Heerdt, and Leonard H. Augenlicht

Department of Oncology, Albert Einstein Cancer Center, Montefiore Medical Center, Bronx, New York 10467

ABSTRACT

The orphan nuclear receptor TR3/Nur77 has emerged as a viable candidate in the coordinate regulation of cell proliferation and apoptosis, essential for maintaining normal architecture in rapidly renewing tissues such as the colonic mucosa. TR3 induces apoptosis in a number of cell lineages exposed to proapoptotic stimuli by directly targeting the mitochondria, inducing cytochrome *c* release. Here we report a distinctly different mechanism of TR3-mediated apoptosis in colon cancer cells. Nucleus-to-cytoplasm translocation of a green fluorescent protein-TR3 construct, but not its direct mitochondrial targeting, was associated with apoptosis induced by the short-chain fatty acid, butyrate. Similar results were observed for the nonsteroidal anti-inflammatory drug, sulindac, and the chemotherapeutic drug, 5-fluorouracil. A mutant TR3 construct lacking DNA-binding ability exerted a potent proapoptotic effect in colon cancer cells that was associated with cytochrome *c* release, an action dependent upon cytoplasmic localization of the construct, but, again, not its direct mitochondrial targeting. We identified a potential role for BAX recruitment to the mitochondria, secondary to cytoplasmic translocation of TR3, in inducing cytochrome *c* release and in mediating apoptosis. Therefore, TR3 translocation from the nucleus may initiate the apoptotic cascade in colon cancer cells by stimulating other cytosolic proapoptotic molecules to associate with mitochondria.

INTRODUCTION

To maintain the architecture of rapidly renewing tissues, such as the colonic mucosa, there must be tightly regulated control of both cell proliferation and apoptosis. The mitochondria has been hypothesized to play a key role in such control (1). Recent evidence indicates that the orphan nuclear receptor TR3 (also called Nur77 or nerve growth factor-induced protein-B), a transcription factor of the steroid/thyroid receptor superfamily with no identified endogenous ligand, can regulate, and perhaps coordinate, cell proliferation and apoptosis in several cell lineages.

TR3 is the product of an immediate-early response gene, the expression of which is induced rapidly by various growth stimuli (2). TR3 is a transcription factor known to modulate gene expression linked to the regulation of cell proliferation and apoptosis (3, 4). An additional role for TR3 in the regulation of cell survival has been identified recently: in prostate, breast, and gastric cancer cells, several inducers of apoptosis stimulate TR3 translocation to the outer mitochondrial membrane, resulting in the release of cytochrome *c* into the cytosol to initiate an apoptotic cascade (4, 5). An important feature of this cytoplasmic localization is the possibility that it plays a key role in coordinating growth and apoptotic pathways through the cessation of the transcriptional program mediated by TR3 after its translocation from the nucleus.

We demonstrated that the role TR3 plays in the apoptotic response of colon carcinoma cells appears to be distinctly different from that reported in prostate cancer cells. While nucleus-to-cytoplasm translocation of a full-length GFP[3]-TR3 construct accompanies apoptosis that is induced in colon cancer cells by the SCFA, butyrate, by the nonsteroidal anti-inflammatory drug, sulindac, and by the chemotherapeutic drug, 5-FU, there appears to be no association with the mitochondria. Additionally, a mutant TR3 construct lacking DNA-binding ability exerted a potent proapoptotic effect that correlated with cytochrome *c* release that was mediated, at least in part, through relocalization of the proapoptotic Bcl2 family member, BAX, to the mitochondrial membrane. However, similar to butyrate-stimulated translocation of the full-length TR3 construct into the cytoplasm, no direct mitochondrial targeting of this mutant construct was observed. Thus, although TR3 translocation from the nucleus may be an apoptotic signal for colon cancer cells, it appears that the mitochondria are not targeted directly. Instead, the trigger for the apoptotic cascade may involve recruitment of other proapoptotic molecules.

MATERIALS AND METHODS

Cell Culture. HCT116 cells with and without deletion of both *p53* alleles were kind gifts from Dr. Vogelstein (The Johns Hopkins Oncology Center, Howard Hughes Medical Institute, Baltimore, MD; Ref. 6). Two other colon cancer cell lines, Caco-2 and HCT15, were obtained from ATCC (Manassas, VA). All were maintained by serial passage at 37°C, 5% CO_2 in MEM supplemented with 10% fetal bovine serum, 1× antibiotic/antimycotic (100 units/ml streptomycin sulfate, 100 units/ml penicillin G sulfate, and 0.25 μg/ml amphotericin B), 100 μM nonessential amino acids, and 10 mM HEPES buffer solution (all from Invitrogen, Carlsbad, CA). LNCaP prostate cancer cells were also obtained (ATCC) and maintained in RPMI 1640 (ATCC) supplemented with 10% fetal bovine serum (Invitrogen).

Reagents. Two constructs, a GFP-TR3 fusion protein and a conjugated TR3 mutant lacking the DBD (GFP-TR3/DBD), were kind gifts from Dr. Zhang (The Burnham Institute, La Jolla, CA; Ref. 5). An integral membrane GFP marker, Us9-GFP (a kind gift from Dr. Enquist, Department of Molecular Biology, Princeton University, Princeton, NJ; Refs. 7 and 8), was used to test whether effects ascribed to TR3 were specific rather than nonspecific consequences of GFP expression in the cells. These constructs were transfected into subconfluent monolayers using the Lipofectamine Plus transfection system (Invitrogen). The sodium salt of the SCFA, butyrate, the phorbol ester TPA, and the inhibitor of nuclear protein export, LMB, were all obtained from Sigma (St. Louis, MO).

Immunofluorescence Analysis. Cells were cultured overnight on preferred glass coverslips (Fisher, Pittsburgh, PA) and then treated with the agents described above, as required. The cells were fixed for 15 min in 4% paraformaldehyde (Electron Microscopy Services, Ft. Washington, PA), permeabilized with 0.5% Triton X-100/PBS for 5 min, and then incubated for 1 h in a 1% BSA/PBS blocking solution. To detect mitochondria, a mouse monoclonal Hsp60 antibody was used (Santa Cruz Biotechnology, Santa Cruz, CA; 1:200 dilution), the binding of which was detected by a goat antimouse FITC-conjugated secondary antibody (Roche Diagnostics/Boehringer Mannheim Corporation, Indianapolis, IN). Cytochrome *c* was detected using a mouse monoclonal anti-cytochrome *c* IgG (PharMingen, San Diego, CA; 1:200 dilution), followed by exposure to a goat antimouse Cy5-conjugated secondary antibody (Amersham Biosciences, Piscataway, NJ). To detect BAX, cells were incubated for 3 h with a rabbit polyclonal IgG recognizing the NH_2 terminus of the protein (Upstate Biotechnology, Lake Placid, NY; 1:100 dilution),

Received 04/03/03; revised 6/4/03; accepted 06/17/03.

The costs of publication of this article were defrayed in part by the payment of page charges. This article must therefore be hereby marked *advertisement* in accordance with 18 U.S.C. Section 1734 solely to indicate this fact.

[1] Supported by Grants CA81326, CA92713, and PO 13330.

[2] To whom requests for reprints should be addressed, at Albert Einstein Cancer Center, Department of Oncology, Montefiore Medical Center, Hofheimer 509, 111 East 210th Street, Bronx, NY 10467. Phone: (718) 920-2093; Fax: (718) 882-4464; E-mail: awilson@montefiore.org.

[3] The abbreviations used are: GFP, green fluorescent protein; SCFA, short-chain fatty acid; 5-FU, 5-fluorouracil; ATCC, American Type Culture Collection; DBD, DNA-binding domain; TPA, 12-*O*-tetradecanoylphorbol 13-acetate; LMB, leptomycin B; Hsp60, heat shock protein 60; ER, endoplasmic reticulum; FACS, fluorescence-activated cell sorter; DAPI, 4′,6-diamidino-2-phenylindole.

followed by exposure to a goat Cy3-conjugated antirabbit secondary antibody (Amersham). Also used were a rabbit polyclonal antibody recognizing calnexin, a protein found in the outer membrane of the ER (Santa Cruz Biotechnology; 1:100 dilution), and a mouse monoclonal antibody raised against the Golgi 58K protein, a microtubule-binding protein that resides in the peripheral membrane of the Golgi apparatus (Sigma; 1:50 dilution). All secondary antibodies were used at a 1:200 dilution with incubation for 1 h. To visualize nuclei, cells were stained with 1 μg/ml DAPI (Sigma). Cells transfected with the GFP-conjugated constructs were visualized directly in the FITC channel of a BX60 Olympus fluorescence microscope (Olympus, Melville, NY). All images were captured with a SPOT RT Diagnostic Instruments charge-coupled device camera (Diagnostic Instruments, Sterling Heights, MI).

Evaluation of Apoptosis. Apoptosis was assessed initially by flow cytometry, as we have reported previously and validated (9). Cells grown in 6-well plates were treated with butyrate or TPA and assayed in triplicate. After 12-, 24-, or 48-h exposures, both attached and floating cells were harvested, washed in PBS, centrifuged for 5 min at 4°C, and then resuspended in cold PBS containing 50 μg/ml propidium iodide, 0.1% sodium citrate, and 0.1% Triton X-100. After overnight staining at 4°C, the cells were analyzed by flow cytometry (FACScan; Becton Dickinson Immunocytometry Systems, San Jose, CA). The percentage of cells containing subdiploid DNA content, a characteristic of apoptosis, was quantified using WinList 2.0 software (Verity Software House, Inc., Topsham, ME).

Apoptosis was subsequently assessed in 200 cells by nuclear morphology after staining with DAPI. The final method for quantification of apoptotic cells involved scoring the number of cells that were simultaneously exhibiting BAX localization to the mitochondrial membrane and cytochrome *c* release in 200 cells.

Measurement of TR3 mRNA Levels. Steady-state levels of TR3 mRNA in HCT116, HCT15, and LNCaP cells were measured by real-time PCR analysis, as described previously (10). Primer sequences used were: Human TR3 forward, 5′-GCGGTTGTCTGGGACCTTT-3′; and Human TR3 reverse, 5′-GCTTGGATACAGGGCATCTCA-3′.

Statistical Analysis. Statistical significance was assessed using Student's *t* test (Minitab release 8 for the Macintosh; Minitab, Inc., State College, PA). A value of $P \leq 0.05$ compared with untreated cells was considered statistically significant.

RESULTS

Induction of Apoptosis and Expression of TR3. Two agents known to induce apoptosis in a wide variety of cancer cells, butyrate, a physiologically relevant compound for the colonic epithelium, and the phorbol ester TPA (4, 5, 11–13), were used to examine the role TR3 plays in colon cancer cell apoptosis. Because LNCaP prostate cancer cells have been well characterized in terms of their dependence upon TR3 for mediating apoptosis in response to TPA (5), this cell line was included in these analyses as a positive control.

In LNCaP cells (Fig. 1*a*), both butyrate (5 mM) and TPA (10^{-7} M) increased the percentage of cells showing subdiploid content of DNA detected by flow cytometry, although TPA had an earlier and considerably more potent effect than did butyrate. We have confirmed previously that subdiploid DNA content is indicative of apoptosis (Ref. 9 and below). By contrast, only butyrate significantly stimulated apoptosis after 24–48 h of exposure in HCT116 colon cancer cells (Fig. 1*b*). The observation that TPA exerted minimal effects on apoptosis contrasts with previous studies using a wide range of cells of noncolonic epithelial origin (4, 5), but is consistent with a previous report in colon cancer cells (14).

Both LNCaP and HCT116 cells expressed TR3 constitutively, as assessed by real-time reverse transcriptase-PCR analysis of steady-state mRNA levels (Fig. 2). Interestingly, HCT116 cells showed markedly lower basal levels of TR3 expression than the prostate cancer cells. Analysis of two other colon cancer cell lines, HCT15 and Caco-2, revealed a similar relative paucity of basal TR3 expression (data not shown). In both LNCaP and HCT116 cells, the ability of

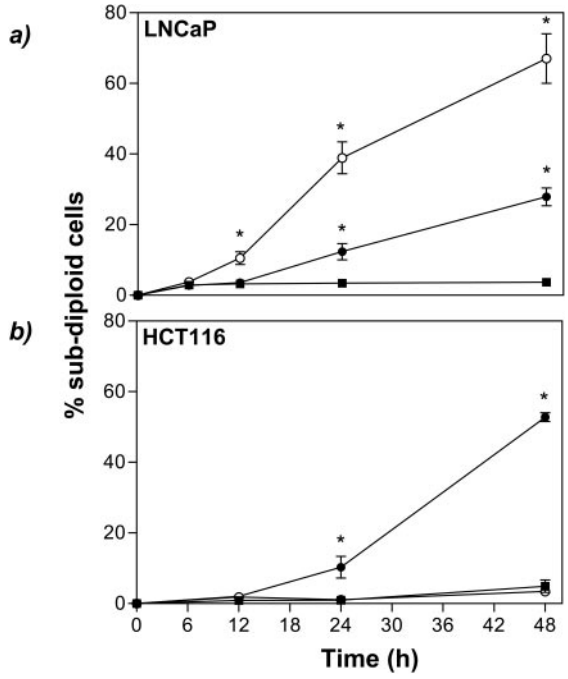

Fig. 1. Induction of apoptosis by butyrate and TPA. Apoptosis was measured by FACS and expressed as the percentage of cells with subdiploid DNA content present in untreated (■) and in 5 mM butyrate (●) or 10^{-7} M TPA (○)-treated subconfluent cell monolayers. *a*, LNCaP prostate cancer cells; *b*, HCT116 colon cancer cells. Values are means of three independent experiments; *bars*, SE. *, $P < 0.05$, Student's *t* test.

butyrate and TPA to induce apoptosis correlated with their relative effects on the expression of TR3. As shown in Fig. 2, both agents significantly increased steady-state mRNA levels of TR3 in LNCaP cells after 6 h, with TPA exerting the more potent stimulatory effect. In HCT116 cells, butyrate induced an ~2.5-fold induction of TR3 expression after a 12-h incubation, consistent with its proapoptotic activity. By contrast, TPA did not significantly alter steady-state TR3 levels after this time, consistent with the lack of effect of TPA on apoptosis in this cell line.

Induction of Apoptosis by a TR3 Construct Lacking DNA-binding Ability. As reported previously, a construct designated GFP-TR3/DBD, which has a deletion of the DNA-binding domain of TR3, potently induces apoptosis in LNCaP cells (5). We therefore tested its effect on apoptosis in colon cancer cells. This construct and a full-length GFP-TR3 construct were visualized by fluorescence microscopy. Additionally, a construct containing GFP fused with an unrelated protein, the integral membrane protein Us9 (Us9-GFP; Refs. 7 and 8), was also transfected to test the specificity of the effects ascribed to TR3. Apoptotic cells were quantified by DAPI staining 48 h after transfection of the constructs.

We confirmed that the GFP-TR3/DBD construct induced ~35% of LNCaP cells expressing detectable GFP to undergo apoptosis (Fig. 3), as was consistent with previous results (5). Analysis of HCT116 cells transfected with GFP-TR3/DBD revealed that ~40% of transfected cells were apoptotic (Fig. 3), which was of a similar magnitude to GFP-TR3/DBD-induced apoptosis in another colon cancer cell line, HCT15 (data not shown). The potency of apoptosis induction by the mutant construct in HCT116 cells was well in excess of that induced by the wild-type GFP-TR3 construct (Fig. 3) and was comparable with the extent of apoptosis induced by butyrate after 48 h in these cells (Fig. 1*b*). The Us9-GFP fusion construct had no effect on apoptosis in any of the cell lines examined (Fig. 3), indicating that the inability of TR3 to bind to DNA was a specific apoptotic stimulus for both the prostate and colon cancer cells.

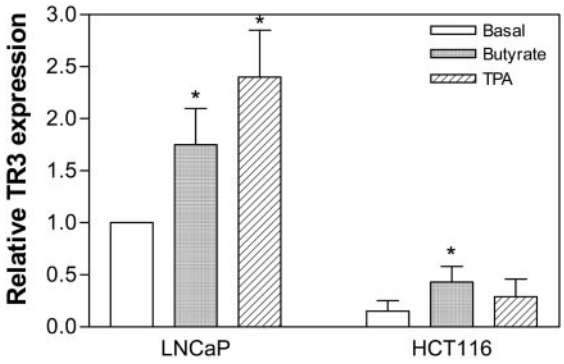

Fig. 2. Effect of butyrate and TPA on TR3 expression. Steady-state mRNA levels of TR3 were quantified by real-time reverse transcriptase-PCR analysis. RNA was collected from cells after the addition of 5 mM butyrate or 10^{-7} M TPA to subconfluent monolayers for 6 h (*LNCaP* cells) or 12 h (*HCT116* cells). Values are expressed relative to TR3 mRNA expression in untreated LNCaP cells and are means of three experiments; *bars*, SE. *, $P < 0.05$ relative to basal levels in the corresponding cell line.

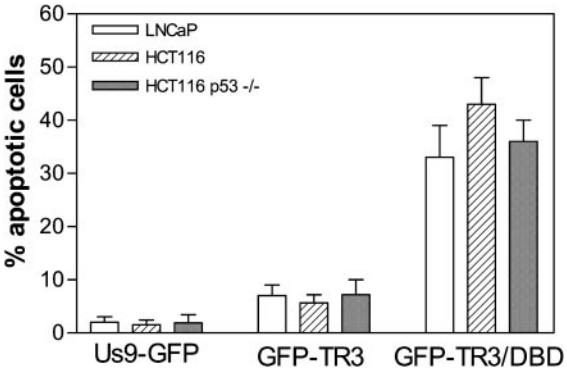

Fig. 3. Effects of TR3 constructs on apoptosis. Apoptotic cells were identified by characteristic nuclear condensation after DAPI staining. LNCaP, HCT116 cells lacking both *p53* alleles (HCT116 *p53* −/−), and *p53* wild-type HCT116 cells were transfected with a full-length *GFP-TR3* construct, a construct lacking DNA-binding ability, *GFP-TR3/DBD*, and a construct containing GFP fused with an unrelated protein, the integral membrane protein Us9 (*Us9-GFP*). These counts were expressed as a percentage of apoptotic cells detected per 200 nuclei examined 48 h after transfection with the constructs. Only cells that expressed detectable GFP were counted. Values are means of three independent experiments; *bars*, SE.

To explore the role of *p53* in GFP-TR3/DBD-induced apoptosis, we used HCT116 cells with deletion of both *p53* alleles (6). As shown in Fig. 3, a similar level of apoptosis induction by the GFP-TR3/DBD construct was detected in HCT116 cells lacking *p53* (HCT116 *p53* −/−) as that observed in the *p53*-wild-type HCT116 cells used throughout these studies. Therefore, the proapoptotic effect of TR3 mediated through its inability to bind to DNA was *p53* independent.

Translocation of Nuclear TR3 in Response to Apoptotic Stimuli. A potential role for TR3 in the proapoptotic effect of butyrate in LNCaP and HCT116 cells was suggested by the apoptosis and TR3 expression studies described above. It has been demonstrated previously that increased expression of TR3 and its subsequent translocation to the mitochondrial membrane are hallmarks of apoptosis induction by various stimuli (4, 5).

After transfection with the full-length GFP-TR3 construct, fluorescent immunolocalization studies were performed in untreated LNCaP cells and in cells treated with TPA (10^{-7} M) or butyrate (5 mM). In control, untreated LNCaP cells (Fig. 4*a*), GFP-TR3 exhibited a diffuse staining pattern that was exclusively nuclear in localization. As reported previously (5), TPA induced a rapid translocation of GFP-TR3 to the mitochondria in LNCaP cells (Fig. 4*b*). Within 1 h of its addition, we observed a bright punctate GFP-TR3 staining pattern that localized exclusively to the cytoplasm. Costaining with an antibody against mitochondrial Hsp60 revealed complete overlap between GFP-TR3 and the mitochondria after TPA treatment.

In LNCaP cells, butyrate also induced mitochondrial targeting of GFP-TR3, as shown in Fig. 4*c*. By 8 h after butyrate exposure, ~15% of transfected cells displayed a similar punctate cytoplasmic GFP-TR3 staining pattern as that described above in TPA-treated cells. Therefore, the time course of the mitochondrial targeting of GFP-TR3 induced by butyrate was delayed compared with that of TPA, consistent with the relative kinetics of their effects on apoptosis induction in LNCaP cells (Fig. 1*a*).

Fluorescent localization studies were also done in HCT116 cells transfected with the GFP-TR3 construct, and then treated for various times (6–48 h) with the same concentrations of butyrate and TPA as those used in the studies using LNCaP cells. Four distinct staining patterns for the GFP-TR3 construct were observed: exclusive nuclear localization (Fig. 5*a*), nuclear localization as well as diffuse cytoplasmic expression (Fig. 5*b*), exclusive cytoplasmic expression in a punctate pattern (Fig. 5*c*), and expression surrounding condensed nuclei, characteristic of apoptosis (Fig. 5*d*). The photomicrographs show the spectrum of GFP-TR3 localization in cells treated with butyrate for 24 h. Also shown in Fig. 5 is the percentage of transfected cells that exhibited each pattern as a function of time after treatment. Two hundred cells were counted for each treatment, at each time point examined.

Under basal, unstimulated conditions, >95% of cells revealed an exclusively nuclear localization after 24 h of culture (Fig. 5*a*). This is consistent with our observation in LNCaP cells (Fig. 4*a*) and with previous studies using these and different cell types (4, 5) and, generally, with the role of TR3 as a nuclear transcription factor. Treatment with either butyrate or TPA induced a shift toward TR3 translocation into the cytoplasm, although two important differences were observed between their relative effects:

(*a*) TPA induced a significant increase in cells showing nuclear/cytoplasmic staining (Fig. 5*b*), followed by punctate cytoplasmic staining (Fig. 5*c*), at least 4 h earlier than did butyrate. The relative difference in time course of effect between butyrate and TPA, an activator of the serine/threonine kinase protein kinase C, may reflect the dependence of nuclear export upon phosphorylation of serine 105 in TR3 (15).

(*b*) Although TPA induced a more rapid and more marked cytoplasmic GFP-TR3 translocation than did butyrate, TPA did not induce apoptosis above that of basal levels as did butyrate (Fig. 5*d*), consist-

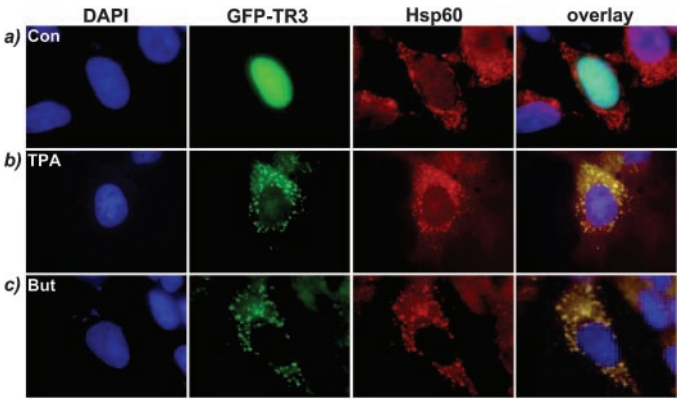

Fig. 4. Association between TR3 and the mitochondria in prostate cancer cells. High-power photomicrographs of LNCaP cells demonstrating localization of GFP-TR3 in relation to DAPI-stained nuclei and mitochondrial Hsp60 in control, untreated cells (*Con*; *a*) and after 1-h treatment with TPA (*TPA*; 10^{-7} M; *b*) or 8-h treatment with butyrate (*But*; 5 mM; *c*).

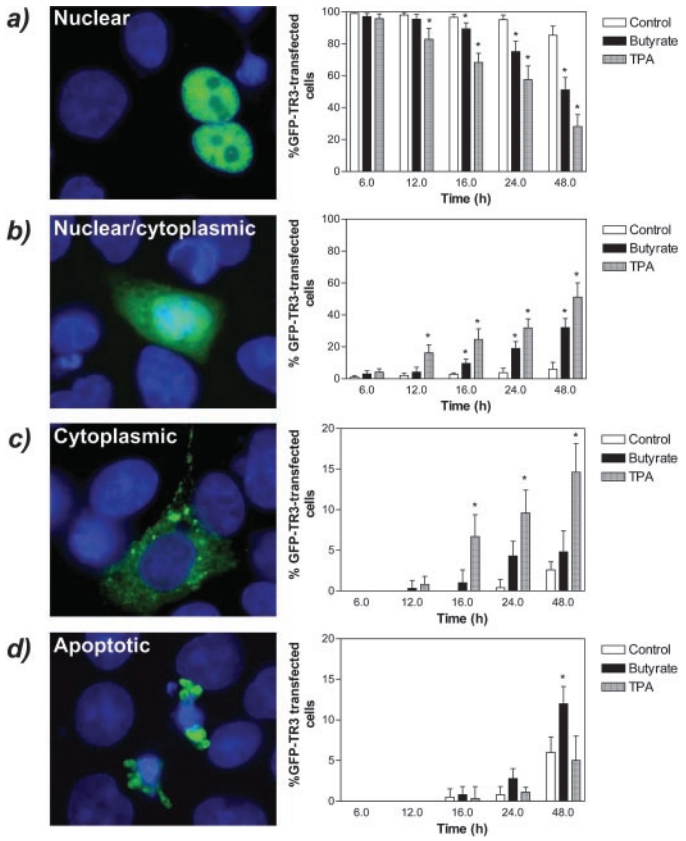

Fig. 5. Localization of the GFP-TR3 construct in HCT116 cells. Fluorescent detection of four distinct staining patterns of the GFP-TR3 construct in untreated cells and in subconfluent monolayers treated with butyrate (5 mM) or TPA (10^{-7} M) for various times. The high-power photomicrographs show the spectrum of GFP-TR3 localization in cells treated with butyrate for 24 h. *a*, exclusively nuclear localization. *b*, diffuse nuclear/cytoplasmic staining. *c*, punctate cytoplasmic staining. *d*, TR3 surrounding condensed nuclei, characteristic of apoptosis. Values were obtained from counts of 200 cells and are expressed as means of three independent experiments; *bars*, SE. $*$, $P < 0.05$ compared with control, Student's *t* test.

ent with the FACS experiments described earlier (Fig. 1*b*). This indicates that the translocation of TR3 from the nucleus to the cytoplasm in colon carcinoma cells was not a sufficient signal for initiation of the apoptotic cascade (see "Discussion").

In HCT116 cells, colocalization studies were again performed with an antibody against mitochondrial Hsp60. The punctate cytoplasmic staining of GFP-TR3 observed after treatment with butyrate or TPA did not colocalize with Hsp60 at any time point. Representative images of GFP-TR3-transfected and Hsp60-immunostained cells under control, basal conditions (Fig. 6*a*) and after a 24-h exposure to butyrate (Fig. 6*b*) or TPA (Fig. 6*c*) are shown. A similar lack of GFP-TR3 mitochondrial targeting was observed in butyrate- and TPA-treated HCT15 and Caco-2 cells, two additional colon cancer cell lines (data not shown). The lack of mitochondrial targeting of GFP-TR3 in response to apoptotic stimuli contrasts to the effect widely reported in non-colon cancer cells (5), which we reproduced in the present study using LNCaP cells (Fig. 4). These studies were extended to two other factors known to induce apoptosis in colon cancer cell lines, sulindac (16) and 5-FU (9). Although both agents induced translocation of GFP-TR3 from the nucleus to the cytoplasm, neither induced its colocalization with Hsp60 over time points ranging from 6 to 48 h. Representative images for cells treated for 24 h with sulindac (Fig. 6*d*) and 5-FU (Fig. 6*e*) are shown.

Localization of the GFP-TR3/DBD Construct. Similar immunofluorescence studies were performed in HCT116 cells transfected with GFP-TR3/DBD, a construct lacking DNA-binding ability that induced a potent proapoptotic effect in these cells (Fig. 3). No cell that was successfully transfected with the construct displayed exclusively nuclear localization of the construct. Rather, GFP-TR3/DBD was detected simultaneously in both the nucleus and cytoplasm of the majority of cells (~60–70%), whereas the remaining cells displayed an exclusively punctate cytoplasmic staining pattern of the construct.

GFP-TR3/DBD associates constitutively with the mitochondria to induce apoptosis in LNCaP cells (5). However, in HCT116 cells, the cytoplasmic staining of GFP-TR3/DBD observed did not colocalize with mitochondrial Hsp60 from 12 to 48 h after transfection of the construct, despite its proapoptotic effect. A representative example demonstrating lack of colocalization of GFP-TR3/DBD and Hsp60 24 h after transfection is shown in Fig. 6*f*. In HCT116 cells lacking *p53* (HCT116 *p53* −/−), where GFP-TR3/DBD induced a similar level of apoptosis as observed in the *p53* wild-type HCT116 cells, cytoplasmic but not mitochondrial targeting of GFP-TR3/DBD was also observed (data not shown).

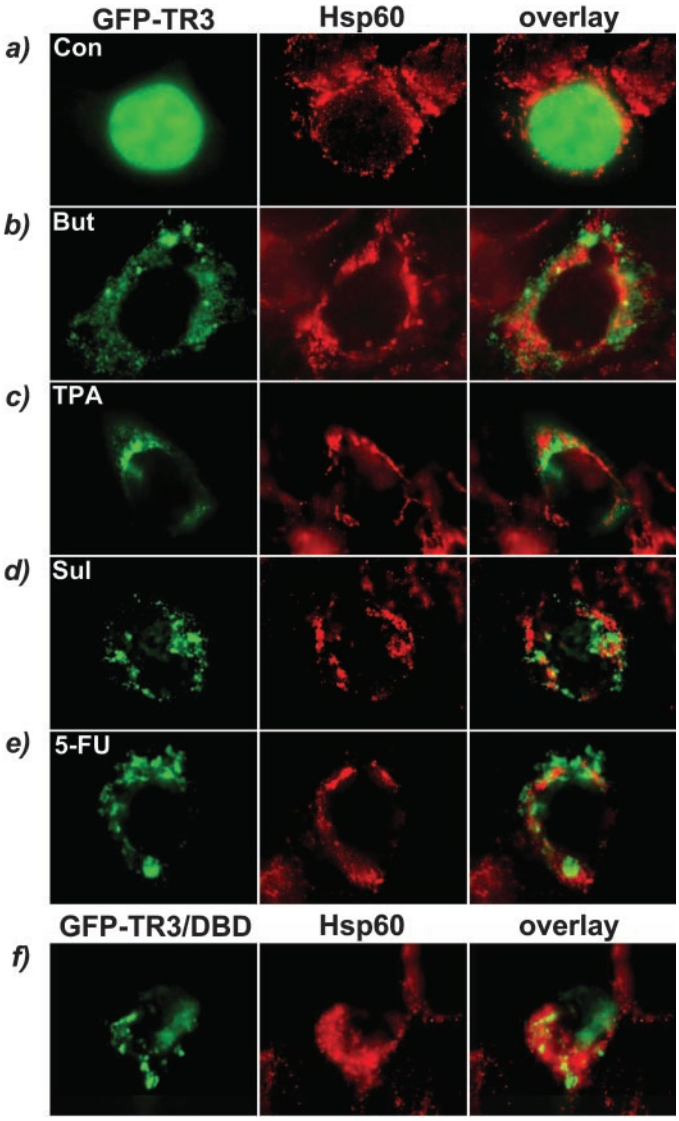

Fig. 6. There was a lack of association between TR3 and the mitochondria in colon cancer cells. High-power photomicrographs of HCT116 cells transfected with either the GFP-TR3 or GFP-TR3/DBD constructs and costained for mitochondrial Hsp60 are shown. *a*, nuclear GFP-TR3 localization in control, untreated cells (*Con*). GFP-TR3 did not colocalize with Hsp60 after 24-h treatment with butyrate (*But*; 5 mM; *b*), TPA (10^{-7} M; *c*), sulindac (*Sul*; 1.6 mM; *d*), or 5-FU (10 μM; *e*). *f* shows that 24 h after transfection of GFP-TR3/DBD, this construct similarly did not target Hsp60.

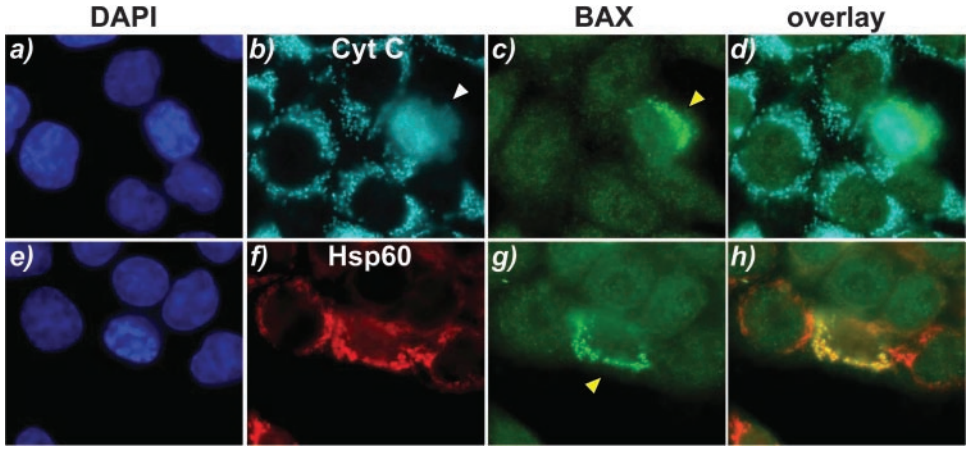

Fig. 7. Detection of cytochrome *c* release and BAX mitochondrial translocation in HCT116 cells. Separate fields of HCT116 cells treated with 5 mM butyrate for 24 h are shown in the *top four* and *bottom four panels*. After butyrate treatment, DAPI-stained nuclei, cytochrome *c* (*Cyt c*),s and BAX (*a–d*) or nuclei, Hsp60, and BAX (*e–h*) were detected. The *white arrowhead* shows a cell releasing cytochrome *c* into the cytosol, whereas the *yellow arrowheads* show cells displaying punctate BAX staining. Punctate BAX staining was shown to be localized to the mitochondria and associated with cytochrome *c* release.

Because the staining of the GFP-TR3/DBD construct in the cytoplasm was of a punctate nature, we explored the possibility that the construct may target other organelles. A role for the ER in mediating apoptosis is well described (17–19). However, the construct failed to colocalize with calnexin, a protein associated with the ER outer membrane (data not shown). Similarly, no overlap was observed between the construct and a Golgi-associated 58K protein (data not shown). A role for the Golgi apparatus in the regulation of apoptosis has been described previously (17, 20).

Cytochrome *c* Release after Transfection with GFP-TR3 or GFP-TR3/DBD. Immunofluorescent detection of cytochrome *c*, a protein localized to the mitochondrial intermembranous space, into the cytosol has been used previously as a marker of an apoptotic cell (4, 5). Fig. 7, *a* and *b*, shows the same field of butyrate-treated cells stained with DAPI and cytochrome *c*, respectively. Two distinct types of cytochrome *c* localization were observed: punctate staining in nonapoptotic cells, which, as expected, colocalized to mitochondrial Hsp60 (data not shown); and diffuse cytoplasmic staining, indicative of cytochrome *c* release from mitochondria, in apoptotic cells (as denoted by the *white arrowhead*).

We quantified the percentage of HCT116 cells transfected with the GFP-TR3 construct that released cytochrome *c* after 24-h treatment with butyrate or TPA. As shown in Fig. 8*a*, butyrate, but not TPA, significantly increased the frequency of cells releasing cytochrome *c* compared with untreated cells. Because butyrate will also induce apoptosis in cells not successfully transfected with GFP-TR3, separate counts were performed on cells within the same monolayer that did not express detectable GFP (data not shown). A similar pattern of effect of induction of cytochrome *c* release by butyrate was observed between transfected and nontransfected cells. The relative effects of butyrate and TPA on cytochrome *c* release were consistent with those observed when apoptosis was assessed by FACS analysis of subdiploid DNA content (Fig. 1*b*) and by nuclear morphology (Fig. 5*d*).

We also quantified the percentage of HCT116 cells transfected with GFP-TR3/DBD that demonstrated cytochrome *c* release. Again, transfected cells and cells that did not successfully take up the construct were counted separately. As shown in Fig. 8*b*, there was a significant enrichment of cells releasing cytochrome *c* in those cells transfected with GFP-TR3/DBD compared with nontransfected cells. Only cells displaying a punctate cytoplasmic staining pattern of GFP-TR3/DBD demonstrated cytochrome *c* release, an effect illustrated in Fig. 9, *a–d*. Therefore, despite the fact that GFP-TR3/DBD did not target the mitochondrial membrane, cytochrome *c* release still underlay the mechanism by which the construct induced apoptosis.

Role of BAX in Cytochrome *c* Release. Because TR3 translocation to the mitochondria did not take place in HCT116 cells and yet its

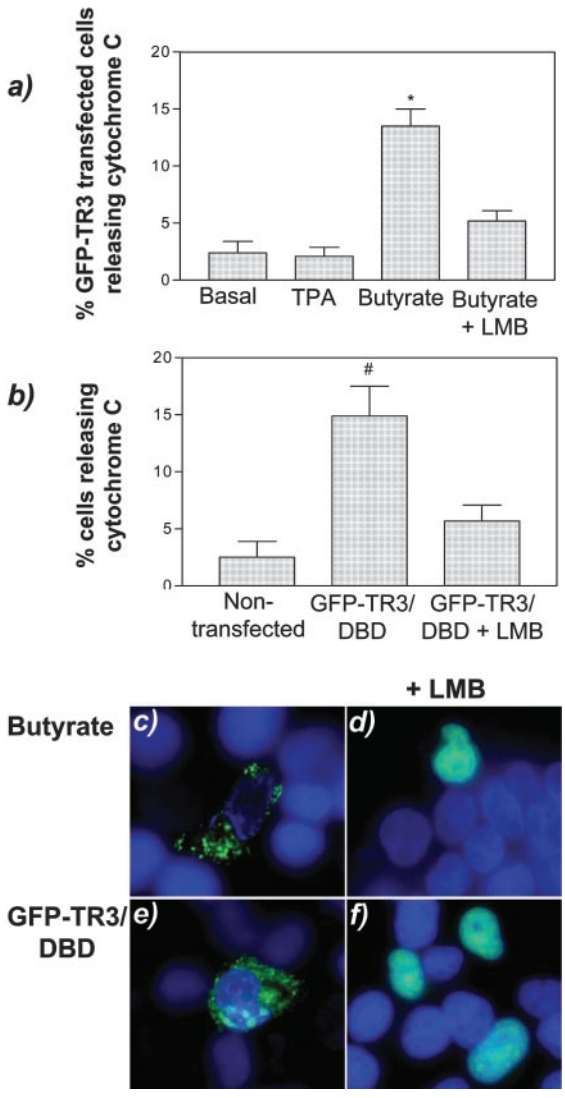

Fig. 8. Quantification of BAX mitochondrial targeting and cytochrome *c* release in HCT116 cells. *a*, after transfection of HCT116 cells with GFP-TR3 and subsequent treatment with butyrate (5 mM) or TPA (10^{-7} M) for 24 h, cytochrome *c* and BAX were detected simultaneously. Only cells that simultaneously showed punctate BAX staining and cytochrome *c* release were counted. *b*, a similar process was undertaken in cells transfected with GFP-TR3/DBD. Values were obtained from counts of 200 cells and are expressed as means of three independent experiments; *bars*, SE. *, $P < 0.05$ compared with GFP-TR3-transfected cells without other treatment (basal). #, $P < 0.05$ compared with cells not transfected with GFP-TR3/DBD, Student's *t* test. The cytoplasmic translocation of GFP-TR3 in response to butyrate (*c*) and GFP-TR3/DBD (*e*) was inhibited by 1 ng/ml LMB (*d* and *f*, respectively). The localization of the constructs relative to DAPI-stained nuclei is shown.

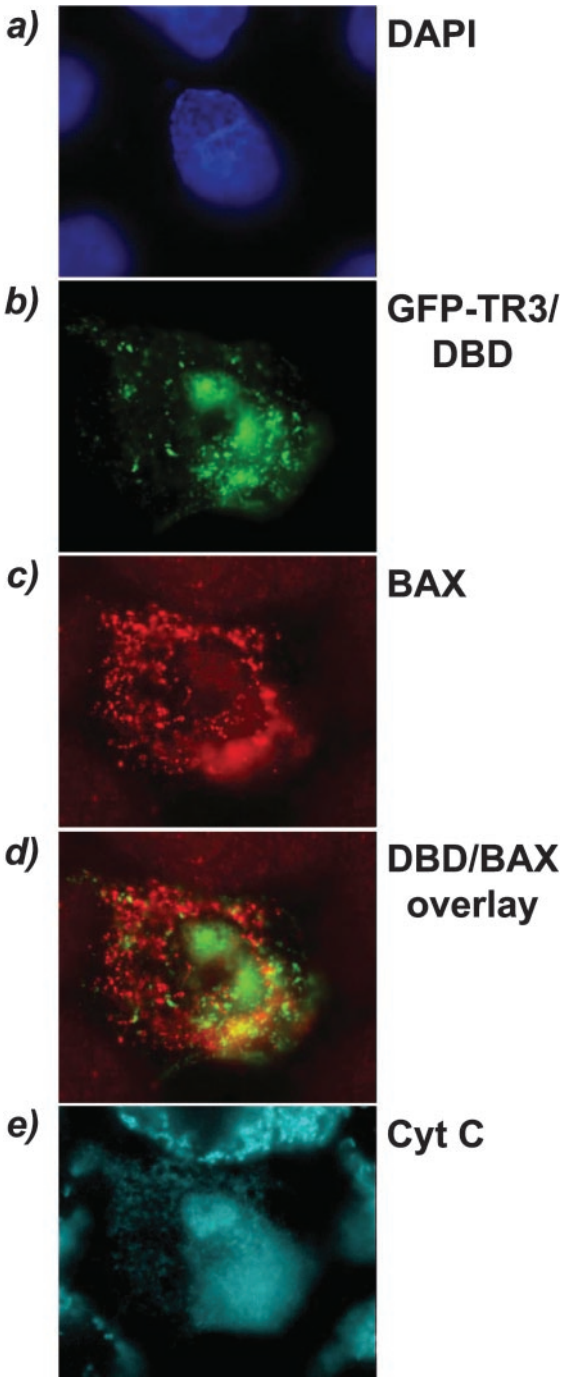

Fig. 9. Cytochrome *c* release and BAX mitochondrial targeting in GFP-TR3/DBD-transfected cells. High-power photomicrographs showing the simultaneous detection of DAPI-stained nuclei, BAX, and cytochrome *c* release in HCT116 cells 24 h after transfection with the GFP-TR3/DBD construct.

cytoplasmic translocation was linked to cytochrome *c* release, we investigated the potential role of BAX. This protein is a member of the Bcl2 family that translocates from the cytosol to the mitochondria in response to proapoptotic stimuli, where it inserts into the mitochondrial outer membrane to facilitate the release of cytochrome *c* (17, 21). Co-incubation experiments were performed with an antibody that recognizes the NH_2 terminus of BAX and the cytochrome *c* or Hsp60 antibodies.

Fig. 7, *c* and *g*, shows separate fields of butyrate-treated HCT116 cells that were stained for BAX. The cells exhibited one of two distinct BAX staining patterns, diffuse cytoplasmic expression or, as designated by the *yellow arrowheads* in each figure, intense punctate staining. Cells exhibiting this punctate BAX staining also displayed cytochrome *c* release into the cytosol (Fig. 7, *b–d*), which suggested that we had detected BAX that had translocated to the mitochondria to effect the apoptotic cascade. This was confirmed in a separate colocalization experiment with the Hsp60 antibody, where clear overlap between punctate, but not diffuse, BAX staining and the mitochondria was observed (Fig. 7, *f–h*). Approximately 8% of butyrate-treated cells showed punctate BAX staining after 24 h. In contrast, <1% of untreated HCT116 cells displayed this pattern of BAX staining after this time, consistent with the very low level of spontaneous apoptosis quantified by FACS (Fig. 1*b*) or by counting DAPI-stained nuclei (Fig. 5*d*).

Cytochrome *c* release was never detected without clear BAX relocalization in HCT116 cells, irrespective of treatment. Therefore, the cell counts presented in Fig. 8 reflect the percentage of cells simultaneously displaying BAX relocalization to the mitochondria and cytochrome *c* release after transfection with GFP-TR3 and/or treatment with butyrate or TPA, or transfection with GFP-TR3/DBD. Several conclusions were drawn from these results: (*a*) the low level of apoptosis observed under basal conditions did involve spontaneous translocation of BAX to the mitochondria; and (*b*) BAX relocalization was an important component of the mechanism of butyrate-induced apoptosis (Fig. 8*a*), an effect illustrated in Fig. 7. Additionally, the recruitment of BAX to the mitochondria after transfection with GFP-TR3/DBD mediated, at least in part, the proapoptotic effect of this construct (Fig. 8*b*), an effect illustrated in Fig. 9. The construct did not significantly colocalize with BAX (Fig. 9, *b–d*), additional evidence that GFP-TR3/DBD did not target the mitochondria.

To further explore the relevance of cytoplasmic translocation of TR3 to mitochondrial targeting of BAX, cytochrome *c* release, and apoptosis induction in HCT116 cells, we used a well-characterized inhibitor of nuclear export, LMB (22). We confirmed that butyrate-induced cytoplasmic translocation of GFP-TR3 (Fig. 8*c*) was inhibited by exposure of these cells to 1 ng/ml LMB, a concentration demonstrated previously to be effective (5). A representative example of LMB-induced nuclear retention of GFP-TR3 after butyrate treatment is shown in Fig. 8*d*. Similarly, cytoplasmic targeting of GFP-TR3/DBD (Fig. 8*e*) was inhibited by LMB, an effect illustrated in Fig. 8*f*.

The effects of LMB on apoptosis induction by butyrate and GFP-TR3/DBD were assessed by costaining for BAX and cytochrome *c*. As shown in Fig. 8*a*, LMB markedly reduced the number of cells successfully transfected with GFP-TR3 that underwent apoptosis in response to butyrate. That this may be attributable to, at least in part, the inhibition of butyrate-mediated cytoplasmic translocation of TR3 was suggested by the fact that the proapoptotic effect of GFP-TR3/DBD was similarly abrogated by LMB (Fig. 8*b*). Because LMB is a general inhibitor of nuclear export, we do not as yet have direct evidence that the translocation of BAX to the mitochondria was dependent upon the cytoplasmic targeting of TR3. However, these LMB studies provide indirect evidence of a link between cytoplasmic TR3 localization and apoptosis induction through BAX recruitment in colon cancer cells.

DISCUSSION

In response to proapoptotic factors, a major effect mediated by the TR3 orphan nuclear receptor is the induction of apoptosis through its direct mitochondrial targeting and stimulation of cytochrome *c* release (5). This phenomenon, which is accompanied by up-regulated TR3 expression, has been described in various cell types, such as prostate, breast, and gastric cancer cells (4, 5). Consistent with these studies, the SCFA butyrate, an important physiological regulator of colonic epithelial cell homeostasis

and a factor attributed with chemopreventive activity in the colon (23, 24), induced TR3-mediated apoptosis in LNCaP prostate cancer cells. However, any such role of TR3 in mediating apoptosis in colon cancer cells has not been defined previously.

We show that butyrate increased endogenous TR3 expression in colon cancer cells and stimulated its translocation into the cytoplasm. However, TR3 did not target the mitochondria in these cells or in those treated with other proapoptotic factors for colon cancer cells, such as the nonsteroidal anti-inflammatory drug sulindac [which, similar to butyrate, has been ascribed chemopreventive activity for colon cancer (25)] and the chemotherapeutic drug 5-FU. The observation that GFP-TR3/DBD potently induced apoptosis in colon cancer cells implied, however, that the inability of TR3 to bind to DNA was still an apoptotic stimulus despite the lack of mitochondrial targeting. This was supported by our studies with LMB, which demonstrated that impaired nuclear export was associated with an abrogation of the ability of GFP-TR3/DBD and butyrate to induce apoptosis. Therefore, stimulation of the cytoplasmic translocation of TR3 in colon cancer cells by factors such as butyrate may still play a role in their proapoptotic activities.

The fact that three different inducers of apoptosis in colon cancer cells induced nuclear-to-cytoplasmic translocation of TR3, that the mutant TR3 construct itself stimulated apoptosis, and that the inhibition of nuclear export abrogated apoptosis induced by butyrate and GFP-TR3/DBD strongly argues that TR3 translocation was an important component of the apoptotic response in colon cancer cells. Several possible mechanisms may underlie the cytochrome *c* release from mitochondria that was concomitant with this translocation. The translocation of TR3 from the nucleus to the cytoplasm may down-regulate the "growth" program linked to the activity of TR3 as a transcription factor (2). In addition, we demonstrated a dependence upon cytoplasmic localization of GFP-TR3/DBD for its proapoptotic effect, which was consistent with the independence from *p53* observed. However, because TPA, which did not induce apoptosis in colon cancer cells, also stimulated the movement of TR3 into the cytoplasm, this translocation was not likely a sufficient trigger for initiating the apoptotic cascade. In this regard, we identified a potential role for BAX recruitment to the mitochondria in mediating basal apoptosis and the proapoptotic effect of butyrate in colon cancer cells, consistent with previous reports demonstrating such effects of Bcl2 family members (21, 26–29). Whether TR3 displaces other proapoptotic cytosolic proteins, such as BAX, from binding partners in order that they target the mitochondria will be the focus of further studies. This will provide insight into other pathways and factors that are necessary for triggering apoptosis in conjunction with TR3 translocation.

There is growing awareness of the considerable complexity of events and of the nature of effectors that mediate cell apoptosis. Our observation that TR3 does not directly target the mitochondria to induce apoptosis in colon cancer cells, in contrast to other cell types, reflects that complexity. The tightly controlled and coordinated regulation of apoptosis and cell proliferation is paramount in preserving normal architecture in rapidly renewing tissues such as the colonic mucosa (1, 30). Therefore, identifying factors that regulate proliferation and apoptosis in the colon are of potential importance in defining mechanisms involved in the development of cancer and/or defining new strategies in cancer chemotherapy or chemoprevention.

REFERENCES

1. Heerdt, B. G., Houston, M. A., Anthony, G. M., and Augenlicht, L. H. Mitochondrial membrane potential ($\delta\psi$(mt)) in the co-ordination of p53-dependent proliferation and apoptosis pathways in human colonic carcinoma cells. Cancer Res., *58:* 2869–2875, 1998.
2. Fahrner, T. J., Carroll, S. L., and Milbrandt, J. The NGFI-B protein, an inducible member of the thyroid/steroid receptor family, is rapidly modified posttranslationally. Mol. Cell. Biol., *10:* 6454–6459, 1990.
3. Weih, F., Ryseck, R. P., Chen, L., and Bravo, R. Apoptosis of Nur77/N10-transgenic thymocytes involves the Fas/Fas ligand pathway. Proc. Natl. Acad. Sci. USA, *93:* 5533–5538, 1996.
4. Wu, Q., Liu, S., Ye, X-F., Huang, Z-W., and Su, W-J. Dual roles of Nur77 in selective regulation of apoptosis and cell cycle by TPA and ATRA in gastric cancer cells. Carcinogenesis (Lond.), *23:* 1583–1592, 2002.
5. Li, H., Kolluri, S. K., Gu, J., Dawson, M. I., Cao, X., Hobbs, P. D., Lin, B., Chen, G-Q., Lu, J-S., Lin, F., Xie, Z., Fontana, J. A., Reed, J. C., and Zhang, X-K. Cytochrome *c* release and apoptosis induced by mitochondrial targeting of nuclear orphan receptor TR3. Science (Wash. DC), *289:* 1159–1164, 2000.
6. Bunz, F., Hwang, P. M., Torrance, C., Waldman, T., Zhang, Y., Dillehay, L., Williams, J., Lengauer, C., Kinzler, K. W., and Vogelstein, B. Disruption of p53 in human cancer cells alters the responses to therapeutic agents. J. Clin. Invest., *104:* 263–269, 1999.
7. Kalejta, R. F., Brideau, A. D., Banfield, B. W., and Beavis, A. J. An integral membrane green fluorescent protein marker, Us9-GFP, is quantitatively retained in cells during propidium iodide-based cell cycle analysis by flow cytometry. J. Exp. Cell Res., *248:* 322–328, 1999.
8. Brideau, A. D., Banfield, B. W., and Enquist, L. W. The *Us9* gene product of pseudorabies virus, an alphaherpesvirus, is a phosphorylated type II membrane protein. J. Virol., *72:* 4560–4570, 1998.
9. Arango, D., Corner, G. A., Wadler, S., Catalano, P. J., and Augenlicht, L. H. c-myc/p53 interaction determines sensitivity of human colon carcinoma cells to 5-fluoruracil *in vitro* and *in vivo.* Cancer Res., *61:* 4910–4915, 2001.
10. Wilson, A. J., Velcich, A., Arango, D., Kurland, A. R., Shenoy, S. M., Pezo, R. C., Levsky, J. M., Singer, R. H., and Augenlicht, L. H. Novel detection and differential utilization of a c-*myc* transcriptional block in colon cancer chemoprevention. Cancer Res., *62:* 6006–6010, 2002.
11. Rothermund, C. A., Kondrikov, D., Lin, M. F., and Vishwanatha, J. K. Regulation of Bcl-2 during androgen-unresponsive progression of prostate cancer. Prostate Cancer Prostatic Dis., *5:* 236–245, 2002.
12. Chopin, V., Toillon, R. A., Jouy, N., and Le Bourhis, X. Sodium butyrate induces P53-independent, Fas-mediated apoptosis in MCF-7 human breast cancer cells. Br. J. Pharmacol., *135:* 79–88, 2002.
13. Heerdt, B. G., Houston, M. A., and Augenlicht, L. H. Potentiation by specific short-chain fatty acids of differentiation and apoptosis in human colonic carcinoma cell lines. Cancer Res., *54:* 3288–3293, 1994.
14. Rickard, K. L., Gibson, P. R., Young, G. P., and Phillips, W. A. Activation of protein kinase C augments butyrate-induced differentiation and turnover in human colonic epithelial cells *in vitro.* Carcinogenesis (Lond.), *20:* 977–984, 1999.
15. Katagiri, Y., Takeda, K., Korinek, V., Yu, Z-X., Ferrans, V. J., Ozato, K., and Guroff, G. Modulation of retinoid signalling through NGF-induced nuclear export of NGFI-B. Nat. Cell Biol., *2:* 435–440, 2000.
16. Bordonaro, M., Mariadason, J. M., Aslam, F., Heerdt, B. G., and Augenlicht, L. H. Butyrate-induced apoptotic cascade in colonic carcinoma cells: modulation of the β-catenin-Tcf pathway and concordance with effects of sulindac and trichostatin A but not curcumin. Cell Growth Differ., *10:* 713–720, 1999.
17. Ferri, K. F., and Kroemer, G. Organelle-specific initiation of cell death pathways. Nat. Cell Biol., *3:* E255–E263, 2001.
18. Zuppini, A., Groenendyk, J., Cormack, L. A., Shore, G., Opas, M., Bleackley, R. C., and Michalak, M. Calnexin deficiency and endoplasmic reticulum stress-induced apoptosis. Biochemistry, *41:* 2850–2858, 2002.
19. Ferrari, D., Pinton, P., Szabadkai, G., Chami, M., Campanella, M., Pozzan, T., and Rizzuto, R. Endoplasmic reticulum, Bcl-2 and Ca^{2+} handling in apoptosis. Cell Calcium, *32:* 413–420, 2002.
20. Garcia-Ruiz, C., Colell, A., Morales, A., Calvo, M., Enrich, C., and Fernandez-Checa, J. C. Trafficking of ganglioside GD3 to mitochondria by tumor necrosis factor-α. J. Biol. Chem., *277:* 36443–36448, 2002.
21. Yu, J., Wang, Z., Kinzler, K. W., Vogelstein, B., and Zhang, L. *PUMA* mediates the apoptotic response to p53 in colorectal cancer cells. Proc. Natl. Acad. Sci. USA, *100:* 1931–1936, 2003.
22. Kudo, N., Matsumori, N., Taoka, H., Fujiwara, D., Schreiner, E. P., Wolff, B., Yoshida, M., and Horinouchi, S. Leptomycin B inactivates CRM1/exportin 1 by covalent modification at a cysteine residue in the central conserved region. Proc. Natl. Acad. Sci. USA, *96:* 9112–9117, 1999.
23. McIntyre, A., Gibson, P. R., and Young, G. P. Butyrate production from dietary fibre and protection against large bowel cancer in a rat model. Gut, *34:* 386–391, 1993.
24. Augenlicht, L. H., Bordonaro, M., Heerdt, B. G., Mariadason, J., and Velcich, A. Cellular mechanisms of risk and transformation. Ann. NY Acad. Sci., *889:* 20–31, 1999.
25. Subbaramaiah, K., Zakim, D., Weksler, B. B., and Dannenberg, A. J. Inhibition of cyclooxygenase: a novel approach to cancer prevention. Proc. Soc. Exp. Biol. Med., *216:* 201–210, 1997.
26. Zhang, L., Yu, J., Park, B. H., Kinzler, K. W., and Vogelstein, B. Role of *BAX* in the apoptotic response to anticancer agents. Science (Wash. DC), *290:* 989–992, 2000.
27. Ruemmele, F. M., Schwartz, S., Seidman, E. G., Dionne, S., Levy, E., and Lentze, M. J. Butyrate induced Caco-2 cell apoptosis is mediated via the mitochondrial pathway. Gut, *52:* 94–100, 2003.
28. Avivi-Green, C., Polak-Charcon, S., Madar, Z., and Schwartz, B. Different molecular events account for butyrate-induced apoptosis in human colon cancer cell lines. J. Nutr., *132:* 1812–1818, 2002.
29. Tong, Y., Yang, Q., Vater, C., Venkatesh, L. K., Custeau, D., Chittenden, T., Chinnadurai, G., and Gordeau, H. The pro-apoptotic protein, Bik, exhibits potent antitumor activity that is dependent on its BH3 domain. Mol. Cancer Ther., *1:* 95–102, 2001.
30. Augenlicht, L. H., and Heerdt, B. G. Mitochondria: integrators in tumorigenesis? Nat. Genet., *28:* 104–105, 2001.
31. The color images in Figures 4–9 can be viewed as high resolution JPEG images on our website: http//sequence.aecom.yu.edu/genome/Publications/.